Millimeterwave Vivaldi Antenna with Liquid Crystal Phase Shifter for Electronic Beam Steering

Matthias Hoefle, Markus Koeberle, Andreas Penirschke, and Rolf Jakoby
Institute of Microwave Engineering and Photonics
Technische Universitaet Darmstadt, 64283 Darmstadt, Germany
Email: hoefle@imp.tu-darmstadt.de

***Abstract*—A new antipodal Vivaldi antenna array element including a liquid crystal (LC) phase shifter for applications within the frequency range of 65 - 110 GHz has been realized. Measured differential phase shift, S-parameters and far field pattern are presented. The integrated liquid crystal phase shifter provides an individual phase adjustment by adapting the LC permittivity with applied bias voltage directly at the finline. A broadband antipodal Vivaldi antenna suits the finline phase shifter design to form the array element. Therefore, the proposed structure offers the potential to be utilized in a wideband array configuration for electronic beam steering.**

I. Introduction

Electronically scanned antenna arrays play a key role in modern steerable antenna array systems, in order to avoid moving parts or rotating mirrors, especially in space. Not only wideband applications like imaging and non-invasive inspection, but also narrowband applications as scanning conveyor belts, satellite communication and automotive radar can profit from electronically scanned antennas. Therefore we are aiming for a compact wideband reconfigurable antenna array with integrated liquid crystal (LC) finline phase shifters (Fig. 1). The phase can be set for each individual array element by applying a bias voltage that orients the LC molecules to a certain angle to the RF field and thus changing the relative permittivity of the medium. Basically any type of transmission line can be applied for the input to form an array. According to this line type a transition to finline needs to be designed. In this paper a rectangular waveguide is chosen as input due to measurement facilities. Besides the transition, the antenna as well as the biasing network have to be designed to complete the array element. Due to its planar structure and the possibility to place the array elements on the same substrate, a large number of elements can be integrated to form a compact array. Although the presented broadband array element covers frequencies from 65 - 110 GHz (extended W-band), the principle is not limited to this frequency band. Since the dissipation factor $\tan\delta$ of LC decreases with frequency [1], the presented antenna configuration is suitable also for frequencies beyond 110 GHz. To further address ongoing projects towards space applications involving liquid crystal devices, LC has already successfully passed first irradiation tests towards space qualification as presented in [2].

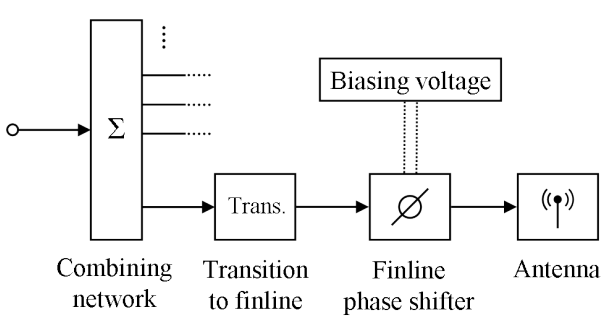

Fig. 1. Block diagram of principle setup of an phased array applying a liquid crystal phase shifter. Parts to design besides the finline phase shifter are the transition to finline, the antenna and the biasing structure for LC orientation.

II. Liquid crystals for microwave and millimeterwave applications

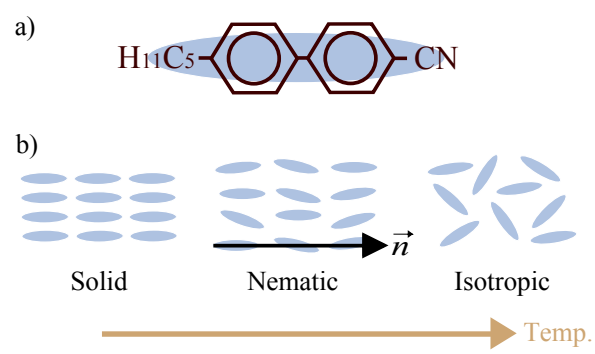

Fig. 2. a) Molecular structure of the common liquid crystal K15 (5CB) and b) its orientational order for the solid, nematic and isotropic phase dependent on its temperature [4].

Liquid crystals (LC), which are well known through modern display technology, are generally formed by one type of two constituents, either rod-like and disk-like organic molecules [3]. One example for an elongated rod-like LC is the compound K15 (5CB), shown in Fig. 2 a [4]. The overall structure has a length of a few nanometers with a permanent dipole moment arising from the CN head. This material also offers great opportunities in the microwave and millimeterwave range and beyond due to its dielectric anisotropy. On the molecule level, depending on the orientation of the RF field relative to the molecule axis orientation, LC materials exhibit dielectric anisotropic behaviour with an overall parallel and orthogonal

permittivity. On the material level, LC molecules offer a variety of phases dependent on the temperature Fig. 2 b. At high temperature the molecules are in an isotropic phase whereas at low temperature the molecules are in a crystalline solid state. One of the essential states, where the molecules show orientational order without positional order, namely nematic phase, is occurring in between. In this state the material is still liquid but with a preferred direction of the molecule axis. This direction is defined as the director $\vec{n}$ in Fig. 2 b. Again dependent on the orientation of the RF field relative to the director $\vec{n}$, LC provides electrically anisotropic behaviour with an overall total continuous tunable permittivity. The orientation of the LC molecules can be controlled by surface treatments as well as by applying static electric or magnetic fields. With a proper design of the electrodes for handling the static electric field, a continuous adjustment of the effective permittivity for the RF field is possible.

In recent years a tremendous effort has been made to improve the properties of liquid crystals in the microwave and millimeterwave range. The main focus lies on the tuning speed as well as on increasing the anisotropy [3] of the compositions, which is defined as

$$\Delta\varepsilon = \varepsilon_{r,\parallel} - \varepsilon_{r,\perp}. \tag{1}$$

Not less important are the efforts towards the reduction of the dielectric losses ($\tan\delta$), utilization at low temperatures and the improvement of the robustness against thermal stress and cosmic radiation. A huge factor for success has been the close cooperation between the group of Microwave Engineering/Institute of Microwave Engineering and Photonics at Technische Universitaet Darmstadt and Merck KGaA as the LC supplier. New mixtures but also well known compositions have been characterized in terms of permittivity and dielectric losses during the optimization process. The resonant cavity perturbation method [5], where LC-filled PTFE tubes are inserted into rectangular waveguide resonators, and the broadband coaxial line method [6], where the material under test affects the electrical properties of a coaxial line, are two developed systems in the microwave range. To characterize LC in the THz range, time-domain THz spectroscopy can be applied [7].

With the developed and characterized liquid crystal compositions various devices for a huge number of applications have been realized in the field of liquid crystal based reconfigurable antenna arrays. Some examples are reconfigurable reflect arrays, inverted microstrip line (IMSL) phase shifters, loaded line phase shifters, LTCC phase shifters and tunable filters as summarized in [4].

In terms of space qualification, a number of LCs have successfully passed first irradiation tests at the Forschungszentrum Juelich [2]. One test scenario has aimed for investigations on the reaction of the material under exposition to photons having a high energy, equivalent to 15 years lifetime of space mission in the low earth orbit. Measured parameters in this study have been the capacitance and conductivity before and after the irradiation. Certain LC mixtures showed only minor changes of the measured parameters and thus proved their suitability.

III. Finline Liquid Crystal Phase Shifter

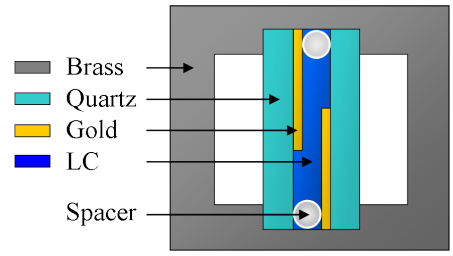

Fig. 3. Layer structure model of LC phase shifter with micro pearl spacers in brass block.

As a key component of the whole reconfigurable antenna array the liquid crystal phase shifter has been designed and optimized in *CST Microwave Studio* as the first step towards the array. As line type an antipodal finline is chosen (Fig. 3). Here almost the whole electrical field is situated inside the liquid crystal which is filled in-between the two parts of the finline. This results in a high tuning efficiency. The first results of this phase shifter have already been published in [8] with promising results. It has been designed with a finline overlap of 110 µm with 100 µm LC layer thickness between two 300 µm thick quartz glasses (Fig. 3). To guarantee the desired distance between the glasses, micro pearls are used as spacers. The gold structures with a thickness of 500 nm are realized with photolithographic processes, namely chrome/gold evaporation, photo resist spin coating, UV exposure, gold plating and gold/chrome etching. A DC tuning voltage between the fins is applied to make use of the dielectric anisotropy of LC. The commercially available LC BL111 from Merck KGaA is taken for the design. This LC has good anisotropy of $\Delta\varepsilon = 0.49$ ($\varepsilon_r = 2.6$ - 3.1) with dielectric losses of $\tan\delta_\perp = 0.022$. Therefore the results can still be improved by applying a high performance LC. To ensure a pre-orientation of the LC molecules a polyimide film is spin coated and rubbed on top of both structured glasses.

An evaluation of phase shifters can be fulfilled by the so-called figure-of-merit (FoM) [2] which is defined by the ratio of the differential phase shift $\Delta\Phi$ and the insertion loss IL of the phase shifter.

$$FoM = \frac{\Delta\Phi}{IL} \tag{2}$$

In [8] a FoM of 10 - 23°/dB from measurements of $\Delta\Phi$ and IL is presented. The phase shift itself is roughly 100° for the designed finline section length of 10 mm. To be able to adjust the individual phase shift of an array element the length certainly has to be increased for the final array design to ensure a minimum phase shift of 360°.

IV. Vivaldi antenna array element

Since the Vivaldi antenna suits the principle layer structure of an antipodal finline (Fig. 3), it can be realized directly

on the same substrates as the finline phase shifter. To verify the functionality of the array element, the finline section and transition from rectangular waveguide can be taken from the phase shifter design. A cross section of the final structure is presented in Fig. 4 and will be further discussed in the next chapter.

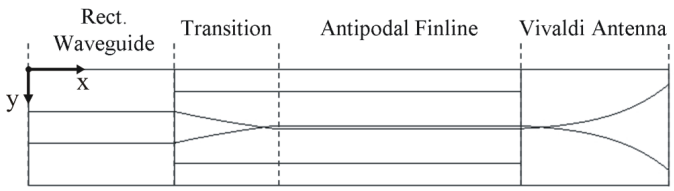

Fig. 4. Array element cross section with the antipodal finline as the phase shifter section, the Vivaldi antenna and the transition from rectangular waveguide.

In order to characterize the realized antenna array element, two main measurement techniques are applied. S-parameter measurements are done for comparing the individual reflections for each biasing voltage. Here also the differential phase shift information can be extracted from measurements with a two port vector network analyzer (VNA). On the other hand far field measurements are fulfilled in an anechoic chamber to compare the element's far field with the simulation results.

A. Design and simulation

The final design of the array element is again done with *CST Microwave Studio*. The Vivaldi antenna itself is designed according to (3), which is derived from [9]. Here x and y form the coordinate system shown in Fig. 4. l is the antenna length, m the shaping coefficient, W the opening width at the antenna end, and w_{fl} the overlapping of the finline.

$$y = \frac{h}{l} x e^{m(l-x)} \tag{3}$$

The height h in (3) is described in (4), representing the opening width at the antenna end, also considering the overlapping w_{fl} of the finline.

$$h = \frac{W + w_{fl}}{2} \tag{4}$$

With the final dimensions of l = 6 mm, W = 3 mm and m = 0.3, the antenna element simulations including the shielding block revealed less than -12 dB of reflection losses for the whole W-band with an antenna gain larger than 8 dB for the relevant permittivity values. Simulations of the complete structure (Fig. 4), including additionally the antipodal finline phase shifter section, the transition and the rectangular waveguide part, showed very promising results [8] with reflections below -7 dB for assumed relative permittivity values from 2.6 - 3.1 of BL111.

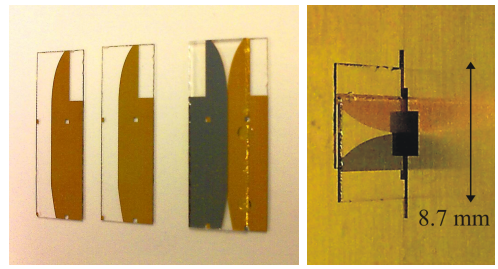

Fig. 5. Left: parts of Vivaldi antenna on quartz glass and glued Vivaldi antenna, right: Vivaldi antenna mounted in brass split block.

B. Realization

The same photolithographic processes as for the phase shifter are applied to realize the array element on 300 µm thick quartz glass. The final element halves are identical as shown in Fig. 5 on the left side. They are assembled with UV glue, mixed with micro pearls with a diameter of 100 µm. The glue is placed next to the glass edges and therefore does not affect the performance of the device's functionality. In the next step aluminum straps for biasing are glued to each of the two element parts with silver epoxy glue. Then the relevant LC mixture is filled into the structure making use of capillary forces. The commercially available LC BL111 from Merck KGaA is again taken for the design. Finally the glued antenna is mounted inside a brass split block with a WR10 waveguide flange on the backside.

Fig. 5 illustrates the realized array element prototype on quartz glass (26 x 8.7 mm), including the Vivaldi antenna as well as the attached finline section for phase shifting (10 mm) and the transition to rectangular waveguide. The right picture in Fig. 5 shows the mounted antenna inside the brass block. Here the overlapping of the two glass pieces is visible.

In Fig. 6 the complete antenna block is shown including the aluminum straps. In between the Vivaldi antenna parts the glass appears a bit milky, which is due to the enclosed liquid crystal. The rectangular waveguide flange on the back side of the split block is connected to the waveguide extension of the VNA.

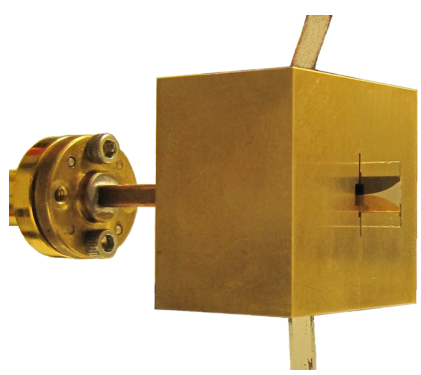

Fig. 6. Realized array element with LC filled glass substrates and aluminum straps for biasing, mounted in brass split block. The antenna block is mounted to the waveguide extension of the VNA.

C. S-parameter measurements

For the S-parameter measurements a two port VNA with waveguide extensions is used. Calibration is done for 65 - 110 GHz up to the waveguide flange of the brass split block to zero cable and waveguide extension influences. First the reflection coefficient is measured without and with bias voltages applied to the two aluminum straps (Fig. 6). The measured reflection coefficient, presented in Fig. 7, is below -7.2 dB for the entire band for zero bias and below -6.1 dB for bias voltages from 2 to 25 V. It it obvious that the change of the permittivity due to applied bias voltage is not significantly affecting the reflection coefficient of the antenna. Therefore it is shown, that the static electric field is not affecting the RF field of the device, although the LC is even situated inside the Vivaldi antenna itself.

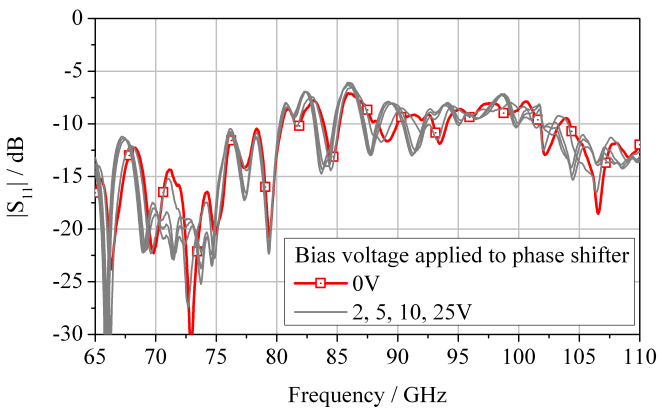

Fig. 7. Measured reflection coefficient $|S_{11}|$ of the realized LC antenna array element with zero bias in comparison to 2, 5, 10 and 25 V applied bias voltage.

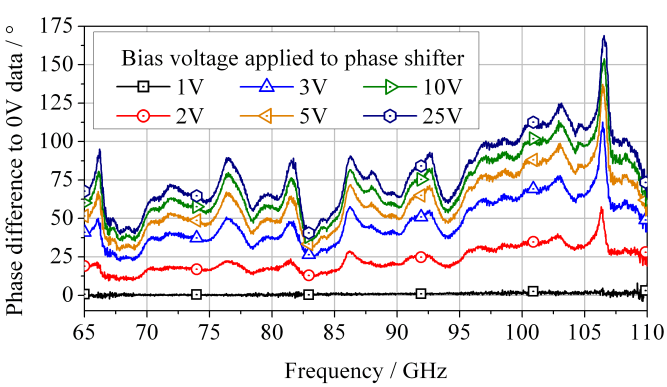

Fig. 8. Measured phase difference or differential phase shift of the Vivaldi antenna array element for bias voltages from 1 - 25 V compared to 0 V reference measurement.

Fig. 8 presents the measured phase difference or differential phase shift of the array element. The phase for zero bias is measured and taken as reference. The measurement results for bias voltages of 1, 2, 3, 5, 10 and 25 V are shown in Fig. 8. With 1 V the voltage is still too low to change to permittivity significantly for the RF field. For 2 V a considerable phase difference to 0 V is measured. For 25 V a minimum differential phase shift of 40° is achieved for the whole extended W-band. At 97 - 108 GHz the differential phase shift is above 100°. The measurement shows that with liquid crystal a continuous broadband tuning of the phase is possible. For frequency bands of special interest the phase shifter can be further optimized. For a final design of the array, the individual differential phase shift needs to be increased by either applying LC with higher anisotropy or/and by increasing the phase shifter length.

D. Far field measurements

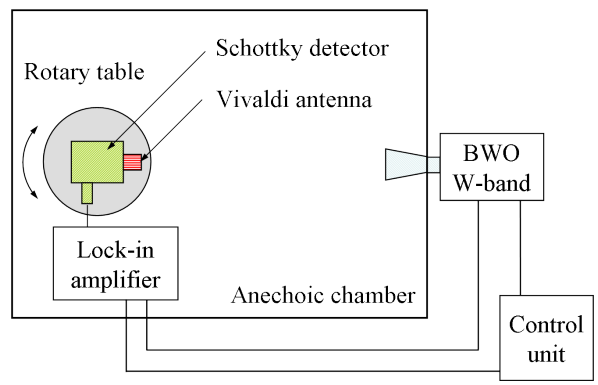

Fig. 9. Far field measurement setup inside an anechoic chamber with BWO source, Schottky detector and log-in amplifier.

Fig. 9 shows the environment of the fulfilled far field measurements in W-band. The setup is placed inside an anechoic chamber, where the Vivaldi antenna block is fixed on a rotary table. The signal strength is measured with a Schottky diode detector. As the signal source a W-band BWO is used. Due to the low signal level at the position of the antenna, an additional lock-in amplifier is implemented in the setup. Measurements in H-plane as well as E-plane with and without liquid crystal are carried out.

An exemplary measurement result of the antenna structure at 100 GHz is shown in Fig. 10. The measurement has been done from -90° to 90° to investigate the antennas forward radiation. The antenna gain is normalized to the maximum

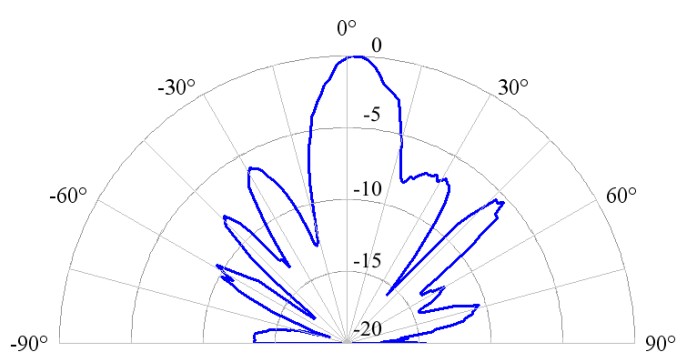

Fig. 10. Normalized antenna gain from far field measurements of forward radiation in E-plane at 100 GHz with LC without biasing voltage.

value. The antenna element is filled with LC BL111 and the measurement has been done without applied bias voltage. A half power beam width (HPBW) of 20° and a side lobe level of -5.5 dB are achieved in E-plane. In simulations, the side lobe level at 100 GHz for the untuned LC ($\varepsilon_r = 2.6$) has been -7.6 dB with an HPBW of 24.7°. The slight asymmetry in the pattern is due to some misalignment in the measurement setup. This typical effect can be observed if the antenna is slightly rotated and shifted vertically, due to the large distance of roughly six meters from the source to the Vivaldi antenna element in the setup. For further measurements a position calibration needs to be implemented to account for this error.

The sealing of the liquid crystal in-between the glass parts has still to be investigated for further designs as well as the array concept. For a first try UV glue is applied at the sides of the glasses to seal the LC. No critical effects have been noticed for the measurements. It is not affecting the far field of the array element, but might add extra losses that could be critical in case of sensitive detector designs.

V. Vivaldi antenna array predictions

The presented antenna structure offers the possibility for implementation as an electronically steerable antenna array by placing additional phase shifters and antennas on the same substrates. Assuming an $\varepsilon_{r,\perp}$ of the LC of 2.6, simulations showed a side lobe level below -10.5 dB, a gain of 16.7 dB and a HPBW of 8.3° of the main lobe for a four element array at 94 GHz. A ten element array configuration offers an angular width of 3.4°. For beam steering the maximum required differential phase shift is accomplished by the length of the phase shifter itself and the required phase is controlled through bias voltages at all antenna elements individually. Steps of 25° phase difference result in a shift of the main beam of 2.5° respectively. 100° phase shift yields a 10° tilt of the main beam in reference to the main beam direction without a phase shift. Coupling effects among the individual elements have shown negligible influence according to simulations in *CST Microwave Studio*.

VI. Conclusion

A new millimeterwave Vivaldi antenna array element is presented. The individual phase adjustment is fulfilled with a liquid crystal antipodal finline phase shifter. The change in phase is achieved by influencing the orientation of the LC molecule with applied bias voltage. Measurements of the array element with the liquid crystal BL111 showed a differential phase shift larger than 100° at 97 - 108 GHz with 25 V biasing voltage. The input reflections are below -6.1 dB for the extended W-band for all tuning states of the LC. In addition far field measurements showed a side lobe level of -5.5 dB with a HPBW of 24.7°. In a further step the antenna element is going to be implemented in a linear array configuration for beam steering.

Acknowledgments

The authors would like to thank CST company for providing the 3D EM simulation software *CST Microwave Studio*, as well as Merck KGaA for providing the liquid crystal samples. The presented work was also supported by the German Research Foundation DFG within the Research Training Group 1037 "Tunable integrated components in microwave technology and optics" (TICMO).

References

[1] S. Mueller, C. Felber, P. Scheel, M. Wittek, C. Hoch, R. Jakoby, "Passive Tunable Liquid Crystal Finline Phase Shifter for Millimeterwaves", *Proc. 35th European Microwave Conf.*, Oct. 2005, pp. 297-300

[2] A. Gaebler, A. Moessinger, F. Goelden, et al., "Liquid Crystal-Reconfigurable Antenna Concepts for Space Applications at Microwave and Millimeter Waves", *International Journal of Antennas and Propagation*, vol. 2009, Article ID 876989, 2009

[3] D.-K. Yang, S.-T. Wu, "Fundamentals of Liquid Crystal Devices", Wiley & Sons, 2006

[4] O.H. Karabey, S. Bildik, C. Fritzsch, S. Strunck, A. Gaebler, R. Jakoby, A. Manabe, "Liquid Crystal Based Reconfigurable Antenna Arrays", *32nd ESA Antenna Workshop*, 2010

[5] A. Penirschke, S. Mueller, P. Scheele, C. Weil, M. Wittek, C. Hock, R. Jakoby, "Cavity perturbation method for characterization of liquid crystals up to 35 GHz," *Proc. 34th European Microwave Conf.*, vol. 2, pp. 545548, Oct. 2004, Amsterdam

[6] O.H. Karabey, F. Goelden, A. Gaebler, R. Jakoby, "Precise Broadband Microwave Material Characterization of Liquids", *European Microwave Conf.*, Sep. 2010, Paris

[7] E.M. Pogson, R. A. Lewis, M. Koeberle, R. Jakoby, "Terahertz Time-Domain Spectroscopy of Nematic Liquid Crystals", Proc. SPIE 7728, 77281Y (2010); doi:10.1117/12.854810

[8] M. Hoefle, M. Koeberle, M. Chen, A. Penirschke, R. Jakoby, "Reconfigurable Vivaldi Antenna Array with Integrated Antipodal Finline Phase Shifter with Liquid Crystal for W-Band Applications", *35th International Conference on Infrared Millimeter and Terahertz Waves*, Sep. 2010, Rome

[9] J. Shin, D.H. Schaubert, "A Parameter Study of Stripline-Fed Vivaldi Notch-Antenna Arrays", *IEEE Transactions on Antennas and Propagtion*, May 1999